

1179W-1340
117-72-CR
308326

P33

AXIONS AND SN 1987A: AXION TRAPPING

Adam Burrows,^a M. Ted Ressel,^{b,c} and Michael S. Turner^{b,c,d}

^aDepartment of Physics and Astronomy
University of Arizona
Tucson, AZ 85721

^bDepartment of Astronomy and Astrophysics
The University of Chicago
Chicago, IL 60637-1433

^cNASA/Fermilab Astrophysics Center
Fermi National Accelerator Center
P.O. Box 500

Batavia, IL 60510-0500

^dDepartment of Physics
Enrico Fermi Institute
The University of Chicago
Chicago, IL 60637-1433

Abstract. If an axion of mass between about 10^{-3} eV and 10 eV exists, axion emission would have significantly affected the cooling of the nascent neutron star associated with SN 1987A. For an axion of mass less than about 10^{-2} eV axions produced deep inside the neutron star simply stream out; in a previous paper we have addressed this case. Remarkably, for an axion of mass greater than about 10^{-2} eV axions would, like neutrinos, have a mean-free path that is smaller than the size of a neutron star, and thus would become "trapped" and radiated from an "axion sphere." In this paper we treat the "trapping regime" by using numerical models of the initial cooling of a hot neutron star that incorporate a diffusion approximation for axion-energy transport. We compute the axion opacity due to inverse nucleon-nucleon, axion bremsstrahlung, and then use our numerical models to calculate the integrated axion luminosity, the temperature of the axion sphere, and the effect of axion emission on the neutrino bursts detected by the Kamiokande II (KII) and Irvine-Michigan-Brookhaven (IMB) water-Cherenkov detectors. The larger the axion mass, the stronger the trapping and the smaller the axion luminosity. We confirm and refine the earlier estimate of the axion mass above which trapping is so strong that axion emission does not significantly affect the neutrino burst: Based upon the neutrino-burst duration—the most sensitive "barometer" of axion cooling—we conclude that for an axion mass of greater than about 3 eV axion emission would not have had a significant effect on the neutrino bursts detected by KII and IMB. The present work, together with our previous work, strongly suggests that an axion with mass in the interval 10^{-3} eV to 3 eV is excluded by the observation of neutrinos from SN 1987A.

N91-13976

(NASA-CR-186467) AXIONS AND SN 1987A: AXIUM
TRAPPING (Fermi National Accelerator Lab.)
CSCL 20H
33 P

Unclas
63/72 0308326

I. Introduction

Peccei-Quinn (PQ) symmetry may be the simplest and most compelling extension of the standard $SU(3)_C \otimes SU(2)_L \otimes U(1)_Y$ model. PQ symmetry cures the single blemish on QCD: the strong-CP problem, and predicts the existence—but not the mass—of a new pseudoscalar particle: the axion.¹ A priori the mass of the axion could be anywhere between about 10^{-12} eV and 1 MeV, corresponding to PQ symmetry breaking scales between about 10^{19} GeV and 100 GeV. (The axion mass and PQ symmetry breaking scale are related by $m_a/\text{eV} \simeq 6 \times 10^6 \text{ GeV}/(f_a/N)$; the axion coupling to ordinary matter is proportional to m_a —or equivalently, $(f_a/N)^{-1}$.) A host of astrophysical and cosmological arguments—and a few laboratory searches—have left open but two “windows” for the axion mass: 10^{-6} eV to 10^{-3} eV and about 1 eV to 5 eV (hadronic axion only); see Refs. 2 for an up-to-date review of the “axion window.” One of the most powerful and important constraints to the axion mass is based upon the early cooling of the neutron star associated with SN 1987A. Axion emission can accelerate the cooling of the nascent neutron star and thereby shorten the neutrino burst. In particular, it has been argued that the neutrino bursts detected by the Kamiokande II (KII) and Irvine-Michigan-Brookhaven (IMB) water-Cherenkov detectors would have been significantly shorter than the bursts actually observed if an axion in the mass interval of 10^{-3} eV to 2 eV existed.³ (Many authors have studied the possible effect of axions on the cooling of SN 1987A; Ref. 4 contains a semi-complete bibliography.)

At the temperatures and densities relevant to the hot, newly born neutron star, the dominant process for axion emission (and absorption) is nucleon-nucleon, axion bremsstrahlung (and inverse axion bremsstrahlung): $N + N \leftrightarrow N + N + a$. Axion emission from the nascent neutron star can be divided into two qualitatively different regimes: “freely streaming,” for $m_a \lesssim 0.01$ eV; and “trapping,” for $m_a \gtrsim 0.01$ eV. In the freely streaming regime the axion-mean-free path for absorption is large compared to the size of the neutron star, and axions, once emitted, simply “freely stream” into the vacuum of space. In the trapping regime, axions interact sufficiently strongly that their mean-free path for absorption is small compared to the size of the neutron star; in this case, like neutrinos, they are said to be “trapped” and are effectively emitted from an axion sphere. (The axion sphere is the surface beyond which the probability for an axion to be absorbed is $\exp(-2/3) \simeq 0.5$.)

Neglecting the “back reaction” of axion emission on the cooling of the neutron star, axion emission in the freely streaming regime is simply proportional to the axion-nucleon coupling squared which is proportional to the axion mass squared. In the trapping regime things are more complicated; in the simplest treatment, the axion luminosity is proportional to the fourth power of the temperature of the axion sphere. Based upon a simple analytic model³ (which this work shows to be quite good) it has been argued that the temperature of the axion sphere varies as $m_a^{-4/11}$, so that the axion luminosity in the trapping

regime should vary as $m_a^{-16/11}$. Very roughly then, one expects that as a function of axion mass, the axion luminosity should increase as m_a^2 for $m_a \ll 10^{-2}$ eV, and should decrease as $m_a^{-16/11}$ for $m_a \gg 10^{-2}$ eV (see Fig. 1). From this simple picture, one sees that here should be two “critical” masses for axion emission from SN 1987A: one below which axion emission is acceptable because the axion interacts so weakly; and one above which axion emission is again acceptable because the axion interacts so “strongly.”

The freely streaming regime is relatively simple to treat: A heat sink of magnitude equal to the local axion-emission rate is incorporated into numerical models of nascent neutron star cooling. In previous work we did just that.⁵ Based upon the duration of the neutrino bursts that would have been observed in the KII and IMB detectors we concluded that the “lower mass boundary” is about 10^{-3} eV. (Several other studies are in agreement with our conclusion.⁴) The trapping regime is more difficult to address because in principle one has to treat axion-energy transport in much the same way as one does neutrino-energy transport (or radiative transport in an ordinary star). Based upon a simple analytic model the “upper mass boundary” was estimated to be about 2 eV.³ The existence of the previously mentioned axion window around a few eV depends crucially upon the upper mass boundary: Were it 5 eV rather than 2 eV the window would be closed. Moreover, one experiment to search for axions in this mass range is currently being carried out,⁶ and another has been proposed.⁷ The first involves searching for the photon-line radiation produced by the decays of relic (cosmological) axions;⁶ and the second involves detecting axions emitted by the sun by axion-photon conversion induced by a strong magnetic field.⁷ For this reason, and the general importance of the SN 1987A bound to the axion mass, we are addressing axion transport and emission in the trapping regime.

To preview our results, the window doesn’t “close up.” Based upon the present work we conclude that the upper boundary mass is about 3 eV, rather close to the original estimate of about 2 eV. The present work together with our previous work⁵ strongly suggests that the durations of the neutrino bursts detected by KII and IMB exclude an axion with mass in the interval 10^{-3} eV to 3 eV. We are quick to remind the reader that both mass boundaries depend upon the precise form of the axion-nucleon coupling, as well as the neutron star models and the exact burst-duration exclusion criterion. The mass boundaries are therefore “fuzzy” by about a factor of two or so.

The outline of the rest of the paper is as follows. In the next Section we will calculate the crucial physics input to the problem: the axion opacity (under ordinary circumstances, this would be an oxymoron). In Section III we will derive the equations that govern axion transport and the diffusion scheme that we employ. Section IV is devoted to a discussion of the results of our numerical simulations of axion-cooled neutron stars, and in Section V we summarize and add some concluding remarks.

II. Axion Opacity

As we have discussed above, for an axion mass of greater than about 10^{-2} eV, it is expected that the axion-mean-free path for absorption (at densities and temperatures typical of a newly born neutron star) is less than the radius of a neutron star.³ In this mass regime axions do not simply stream out and one has to calculate the axion luminosity in much the same way one does the photon luminosity in an ordinary star or the neutrino luminosity in a newly born, hot neutron star. To do so one needs to calculate the axion opacity as a function of density, ρ , temperature, T , and the axion energy, E_a . The axion opacity, κ_E , at energy E_a is related to the axion-mean-free path by

$$(\kappa_E \rho)^{-1} \equiv \lambda_a(E_a, \rho, T). \quad (1)$$

In the present circumstance, unlike photon transport in an ordinary star or neutrino transport in a hot neutron star, only absorption is important. This is because each axion line in a Feynman diagram introduces a dimensionless coupling factor of order $m_N/(f_a/N) \sim 10^{-7}(m_a/\text{eV})$, and so processes involving more than one axion are suppressed relative to those involving a single axion by a factor of at least $10^{-14}(m_a/\text{eV})^2$. By far the dominant axion-absorption process is inverse nucleon-nucleon, axion bremsstrahlung ($a + N + N \rightarrow N + N$; N is a neutron or proton).

There are two equivalent methods for computing λ_a . The first, more familiar to a physicist, relies upon the Boltzmann equation. The mean-free path for absorption is related to the attenuation of the phase space density of a stream of axions moving in the z direction:

$$\lambda_a^{-1} \equiv f_a^{-1} \frac{\partial f_a}{\partial z} = \frac{1}{2E_a} \int d\Pi_1 d\Pi_2 d\Pi_3 d\Pi_4 (2\pi)^4 \delta^4(p_a + p_1 + p_2 - p_3 - p_4) \times S |\mathcal{M}|^2 f_1 f_2 (1 - f_3)(1 - f_4), \quad (2)$$

where p_1, p_2, p_3, p_4 and p_a are the nucleon and axion four momenta, the subscripts 1, 2 (3, 4) refer to the incoming (outgoing) nucleons, $d\Pi_i = d^3 p_i / (2\pi)^3 2E_i$ is the Lorentz-invariant phase-space-volume element, f_i are the nucleon-phase-space distribution functions, S is the symmetry factor (a factor of 1/2 for identical nucleons in the initial or final states), and $|\mathcal{M}|^2$ is the matrix-element squared (summed over initial and final spins). Throughout this Section we shall set $\hbar = k_B = c = 1$. For reference, we remind the reader that the axion-nucleon interaction follows from the Lagrangian density

$$\mathcal{L}_{\text{int}} = \dots + (g_{an}/2m_N)(\bar{n}\gamma_\mu\gamma_5 n)\partial^\mu a + (g_{ap}/2m_N)(\bar{p}\gamma_\mu\gamma_5 p)\partial^\mu a,$$

where the axion-nucleon couplings $g_{an} = c_n m_N / (f_a/N)$ and $g_{ap} = c_p m_N / (f_a/N)$, and c_p and c_n are numerical constants of order unity. For more about the axion and its couplings to ordinary matter see Refs. 8. For the derivation of the matrix element squared and the details of carrying out the phase-space integrations see Ref. 9.

The second method for computing λ_a , more familiar to an astrophysicist, relies upon Kirchoff's law (also known as detailed balance or time-reversal invariance) for calculating the opacity,

$$\kappa_E = \frac{j_E}{d\rho_a(T)/dE}, \quad (3)$$

where λ_a is related to κ_E by Eq. (1), j_E is the axion emission rate (at energy E) per gram of material per second per axion energy interval, and

$$\frac{d\rho_a(T)}{dE_a} = \frac{1}{2\pi^2} \frac{E_a^3}{e^{E_a/T} - 1}, \quad (4)$$

is the differential axion energy density for a thermal distribution of axions. (Expression (3) is probably even more familiar when written for photons: $j_\nu = 4\pi\kappa_{\nu a}B_\nu(T)$, where $B_\nu(T) \equiv 2h\nu^3/(e^{h\nu/kT} - 1)c^2$ is the Planck function, $d\rho_\gamma/d\nu = 4\pi B_\nu/c$, and $\nu = E/h = E/2\pi$ is the frequency; also note that because axions are spinless particles, the Planck functions for photons and axions differ by a factor of 2.) The total *axion-volume-emission rate*, $\dot{\epsilon}_a$ (used in previous work on axions and SN 1987A), is related to j_E by

$$\dot{\epsilon}_a = \rho \int_0^\infty j_E dE_a, \quad (5a)$$

$$\begin{aligned} \dot{\epsilon}_a = & \int d\Pi_1 d\Pi_2 d\Pi_3 d\Pi_4 d\Pi_a (2\pi)^4 \delta^4(p_1 + p_2 - p_3 - p_4 - p_a) E_a \\ & \times S|\mathcal{M}|^2 f_1 f_2 (1 - f_3)(1 - f_4)(1 + f_a). \end{aligned} \quad (5b)$$

To make the calculation of λ_a tractable we will make some approximations. First, we will assume that $|\mathcal{M}|^2$ is approximately constant; as discussed in Refs. 10 this is a reasonable approximation at the temperatures and densities of interest (we will have more to say about this below). Assuming that $g_a = g_{an} = g_{ap}$, $S|\mathcal{M}|^2$ is given by⁹

$$S|\mathcal{M}|^2 = \frac{64}{3} \frac{g_a^2 \alpha_\pi^2}{m_N^2} (3 - \beta) \quad (6a)$$

for $n + n + a \rightarrow n + n$ and $p + p + a \rightarrow p + p$, and

$$S|\mathcal{M}|^2 = \frac{256}{3} \frac{g_a^2 \alpha_\pi^2}{m_N^2} (7 - 2\beta) \quad (6b)$$

for $n + p + a \rightarrow n + p$, where $\alpha_\pi \equiv (fm_N/m_\pi)^2 \simeq 56$ is the nucleon-pion coupling factor and β is a parameter that depends upon the degree of nucleon degeneracy. For completely degenerate nucleon matter $\beta \rightarrow 0$, and for non-degenerate matter $\beta \rightarrow 1.0845$; see the Appendix of Ref. 9 for further details. Next, we assume that the nucleons can be treated as being non-degenerate. Deep in the core this is a marginal approximation;⁹ however further out, near the axion sphere ($T \sim 10$ MeV, $\rho \sim 10^{12} \text{g cm}^{-3}$) where all the action

is, this is a good approximation. (Ishizuka and Yoshimura¹⁰ have recently computed λ_a in the degenerate limit.) We also assume that the nucleons are non-relativistic, which is a very good approximation throughout the star. (In Ref. 11 the fully-relativistic matrix element and phase-space integrations are compared to the non-relativistic matrix element and phase-space integrations.) Finally, in the most important region, that near the axion sphere, the densities are such that many-body effects, e.g., reduction in the effective nucleon mass and variation of the pion-nucleon and axion-nucleon couplings, should not be significant (see Ref. 11). In sum, the ambient conditions near the axion sphere are such that the various approximations we make are well justified.

With these approximations it follows that:

$$f_i = \exp(y_i - u_i), \quad u_i = p_i^2/2m_N T, \quad y_i = (\mu_i - m_N)/T,$$

$$n_i = \frac{1}{\pi\sqrt{2\pi}}(m_N T)^{3/2} e^{y_i},$$

where n_i is the number density of nucleon species i ($= n$ or p) and μ_i is the chemical potential of species i . With these approximations the axion-volume-emission rate for the process $N_1 + N_2 \rightarrow N_3 + N_4 + a$ is given by⁹

$$\dot{\epsilon}_a = \frac{S|\mathcal{M}|^2}{4 \cdot 35 \cdot \pi^{6.5}} m_N^{1/2} T^{6.5} \exp(y_1 + y_2).$$

It is now straightforward to evaluate analytically expression (2) for λ_a^{-1} :

$$\lambda_a^{-1} = \frac{S|\mathcal{M}|^2}{2^5 \pi^{3/2}} \frac{n_1 n_2}{m^{5/2} T^{1/2}} e^{E_a/T} \left(\frac{T}{E_a} \right) \int_{E_a/2T}^{\infty} du_- u_-^{1/2} (u_- - E_a/2T)^{1/2} e^{-2u_-}. \quad (7)$$

(The integrals in expression (2) for λ_a^{-1} are evaluated in an analogous manner, and using the same notation, as those for $\dot{\epsilon}_a$ are in Ref. 9.) The final integral factor which is a function of E_a/T can be expressed in terms of the modified Bessel function $K_1(x)$:¹²

$$e^{E_a/T} \left(\frac{T}{E_a} \right) \int_{E_a/2T}^{\infty} du_- u_-^{1/2} (u_- - E_a/2T)^{1/2} e^{-2u_-}$$

$$= \frac{1}{4} \left(\frac{T}{E_a} \right) \int_0^{\infty} e^{-x} (x + E_a/T)^{1/2} x^{1/2} dx,$$

$$= \frac{1}{8} \exp(E_a/2T) K_1(E_a/2T) \simeq \frac{1}{4} \frac{T}{E_a} \left(1 + \frac{E_a}{T} \right)^{1/2}, \quad (8)$$

where the second expression is a useful empirical fit which has an accuracy of about 10%. Note that the axion-mean-free path is relatively insensitive to the axion energy and temperature, and varies roughly as

$$\lambda_a \propto T^{1/2} \frac{E_a/T}{(1 + E_a/T)^{1/2}}; \quad (9)$$

this is in agreement with the original estimate made in Ref. 3. Note too that the inverse of the axion-mean-free path is proportional to the target-number density squared, rather than the target-number density; this of course is because the absorption process has a three-body initial state with two target nucleons.

Because the axion is a boson, the presence of ambient axions will lead to stimulated emission of axions, *cf.* the factor of $(1 + f_a)$ in Eq. (5). Owing to this fact, the “net” absorption (= true absorption less stimulated emission) is less than the true absorption calculated above, and a “reduced” absorption opacity is often defined. Assuming an ambient thermal distribution of axions, the reduced absorption opacity is

$$\kappa_E^* \equiv \kappa_E \left(1 - e^{-E_a/T}\right). \quad (10)$$

The quantity κ_E^* describes the net axion absorption as a flux of axions passes through matter. As one can readily see the reduced absorption opacity and the absorption opacity do not differ by a large factor since the typical axion energy $E_a \sim 3T$. It is also useful to define the Rosseland-mean opacity

$$\left\langle \frac{1}{\kappa} \right\rangle_R \equiv \int_0^\infty \frac{1}{\kappa_E^*} \frac{\partial^2 \rho_a(T)}{\partial E \partial T} dE / \int_0^\infty \frac{\partial^2 \rho_a(T)}{\partial E \partial T} dE, \quad (11)$$

which weights κ_E^* near the peak of the energy flux ($E_a = 4T$). Using the energy dependence of the axion-absorptive opacity computed above, *cf.* Eq. (7), we find numerically that

$$\left\langle \frac{1}{\kappa} \right\rangle_R = \left(\frac{1}{\kappa_E} \right) \Big|_{E_a=4.73T}. \quad (12)$$

In order to compute the total axion opacity one must consider all three absorption processes ($n + n + a \rightarrow n + n$, $p + p + a \rightarrow p + p$, and $n + p + a \rightarrow n + p$); this is accomplished by adding the corresponding expressions for λ_a^{-1} from each process:

$$\lambda_a^{-1}(\text{total}) = \lambda_a^{-1}(nn) + \lambda_a^{-1}(pp) + \lambda_a^{-1}(np); \quad (13)$$

opacities, like the resistances of resistors in series, add. Finally, taking $g_{an} = g_{ap} = g_a = \frac{1}{2}m_N/(f_a/N) \simeq 7.6 \times 10^{-8}(m_a/\text{eV})$ and setting $\beta = 1.0$, we have evaluated $\lambda_a^{-1}(\text{total})$ numerically:

$$\begin{aligned} \lambda_a^{-1} &= (4.8 \times 10^3 \text{ cm})^{-1} \left(\frac{m_a}{\text{eV}} \right)^2 \left(\frac{T}{\text{MeV}} \right)^{-1/2} \left(\frac{\rho}{10^{14} \text{ g cm}^{-3}} \right)^2 \\ &\quad \times (1 + 8X_n X_p) e^{E_a/2T} K_1(E_a/2T); \end{aligned} \quad (14a)$$

$$\lambda_a^{-1} \simeq (2.4 \times 10^3 \text{ cm})^{-1} \left(\frac{m_a}{\text{eV}} \right)^2 \left(\frac{T}{\text{MeV}} \right)^{-1/2} \left(\frac{\rho}{10^{14} \text{ g cm}^{-3}} \right)^2$$

$$\times (1 + 8X_n X_p) \left(\frac{T}{E_a} \right) \left(1 + \frac{E_a}{T} \right)^{1/2}; \quad (14b)$$

where X_n and X_p are the neutron and proton mass fractions, and in Eq. (14b) we have used our empirical expression for $\exp(E_a/2T)K_1(E_a/2T)$. We have taken $g_{an} = g_{ap} = \frac{1}{2}m_N/(f_a/N)$ for consistency with previous work;⁵ the axion-nucleon couplings depend upon the type of axion—DFSZ or hadronic—the quark distribution functions that are assumed (because of the γ_5 couplings, it is the fraction of the nucleon spin carried by quarks that is relevant—and still uncertain). As we will remind the reader in our concluding remarks, our results depend upon the assumed values of the couplings—and can be re-scaled for different assumed values of the axion-nucleon couplings. From Eqs. (14) we can compute the axion opacity at energy E_a

$$\begin{aligned} \kappa_E = 2.1 \times 10^{-18} \left(\frac{\text{cm}^2}{\text{g}} \right) \left(\frac{m_a}{\text{eV}} \right)^2 \left(\frac{T}{\text{MeV}} \right)^{-1/2} \left(\frac{\rho}{10^{14} \text{gcm}^{-3}} \right) \\ \times (1 + 8X_n X_p) e^{E_a/2T} K_1(E_a/2T); \end{aligned} \quad (15a)$$

$$\begin{aligned} \kappa_E \simeq 4.2 \times 10^{-18} \left(\frac{\text{cm}^2}{\text{g}} \right) \left(\frac{m_a}{\text{eV}} \right)^2 \left(\frac{T}{\text{MeV}} \right)^{-1/2} \left(\frac{\rho}{10^{14} \text{gcm}^{-3}} \right) \\ \times (1 + 8X_n X_p) \left(\frac{T}{E_a} \right) \left(1 + \frac{E_a}{T} \right)^{1/2}. \end{aligned} \quad (15b)$$

Finally, we can compute the Rosseland-mean opacity; using Eq. (12) we find:

$$\langle \kappa \rangle_R \simeq 1.95 \times 10^{-18} \left(\frac{\text{cm}^2}{\text{g}} \right) \left(\frac{m_a}{\text{eV}} \right)^2 \left(\frac{T}{\text{MeV}} \right)^{-1/2} \left(\frac{\rho}{10^{14} \text{gcm}^{-3}} \right) (1 + 8X_n X_p). \quad (15)$$

Of the approximations made in calculating the axion opacity—non-degenerate and non-relativistic nucleons, and constant matrix element squared—the latter is least well justified. Because of the various pion-propagator factors that enter in the matrix element squared, $|\mathcal{M}|^2$ is not constant. The dependence upon the nucleon-momentum transfer enters in the form of the following pion-propagator factors:

$$|\vec{k}|^4/(|\vec{k}|^2 + m_\pi^2)^2, \quad |\vec{l}|^4/(|\vec{l}|^2 + m_\pi^2)^2, \quad |\vec{k}|^2 |\vec{l}|^2 / (|\vec{k}|^2 + m_\pi^2)(|\vec{l}|^2 + m_\pi^2);$$

see Ref. 9. Here $m_\pi = 135$ MeV is the pion mass, and $k = p_2 - p_4$ and $l = p_2 - p_3$ are the four-momenta transfers in the two types of Feynman diagrams (for details, see Ref. 9). The three-momenta exchanged are $|\vec{k}|^2 \sim |\vec{l}|^2 \sim 3m_N T$; at high temperatures, $T \gg m_\pi^2/3m_N \simeq 6$ MeV, the pion-propagator factors become momentum independent and equal to unity. Deep inside the core, the temperatures are sufficiently high that the pion-propagator factors can be ignored; further out—say near the axion sphere where $T \sim 10$ MeV—the validity of ignoring the pion-propagator factors is less justified.

To be more quantitative about the effect of the pion propagator we have computed the axion-emission rate with a pion-propagator factor included, j_E^{PP} , by multiplying the constant matrix element squared by $|\vec{k}|^4/(|\vec{k}|^2 + m_\pi^2)^2$, and comparing it to the rate computed without the pion-propagator factor—the canonical assumption. (We note that this procedure is not precisely correct, as the pion-propagator factor that occurs in the interference terms in $|\mathcal{M}|^2$ involves both $|\vec{k}|$ and $|\vec{l}|$ —see Ref. 9; however, this procedure should give one a pretty good idea of the effect of the pion propagator.)

The ratio of the pion-propagator corrected rate to the uncorrected rate is given by

$$R(\alpha, T) = \frac{\int_0^\infty e^{-x} [(x + \alpha)^{1/2} x^{1/2} (1 + 4\epsilon^2/y_+ y_-) - \epsilon \ln(y_+/y_-)] dx}{\int_0^\infty e^{-x} (x + \alpha)^{1/2} x^{1/2} dx}, \quad (16)$$

where $\alpha = E_a/T$, $\epsilon = m_\pi^2/2m_N T$, and $y_\pm = [(x + \alpha)^{1/2} \pm x^{1/2}]^2 + 2\epsilon$. The axion-emission reduction factor R is shown as a function of temperature in Fig. 2 for $E_a/T = 1, 4, 7$, and 10. For $E_a/T = 4$ (a characteristic value for a thermal distribution and for the Rosseland mean) and $T > 10$ MeV, R is greater than about 1/2. Since $\kappa_E \propto j_E$, R is a measure of the reduction in both axion emission and axion opacity due to the effect of pion propagators in the matrix element squared.

It is straightforward to show that R has the following limiting behaviors: $R \rightarrow 1 - \mathcal{O}(\epsilon)$ for $\epsilon \rightarrow 0$ and $R \rightarrow \epsilon^{-2}$ for $\epsilon \gg 1$. Motivated by this we have used the following expression to approximate R :

$$R(\alpha, T) = \frac{1}{1 + a(\alpha)\epsilon + b(\alpha)\epsilon^2}.$$

For $\alpha = E_a/T = 4$, $a = 0.814$ and $b = 0.054$ give the correct limiting behaviours and a fit that is accurate to better than 7% for all values of T . (For reference, $a = 1.027$, $b = 0.0673$ for $\alpha = 3$ and $a = 2.22$, $b = 0.107$ for $\alpha = 1$.) Although the effect of including the pion propagators is small (see end of Section IV), we have used the above fit to R for $\alpha = 4$ to correct both $\dot{\epsilon}_a$ and κ_E for use in the numerical models in Section IV.

III. Axion-Energy Transport

To properly treat the effects of axions upon the cooling of the nascent neutron star associated with SN1987A in the trapping regime ($m_a \gtrsim 10^{-2}$ eV) one must employ the full apparatus of radiative-transfer theory. This is a formidable task, and in light of all the uncertainties involving in setting a limit to the axion mass—neutron star equation of state, the initial state of the hot neutron star, and the imprecision of our “exclusion criterion” based upon the length of the neutrino burst, we have opted to use an approximation scheme—diffusion—to describe the transport of axion energy out of the newly born neutron star.

Axion transport in SN 1987A is very similar to photon (radiative) transport in an ordinary star, and so we will adopt the language and machinery that has been developed

for that problem. (For the most part we follow the notation and conventions used in Refs. 13, except we use the axion energy E instead of the axion frequency ν .) The primary quantities of interest are the various moments of the specific intensity, I_E . The specific intensity describes the flow of energy carried by axions (dE_a) in a particular direction (\hat{n}) through an area (dA) into a solid angle ($d\Omega$) per energy interval ($dE = h d\nu$) per time (dt),

$$I_E = \frac{dE_a}{\cos\theta dA d\Omega dE dt},$$

where θ is the angle between dA and \hat{n} . The specific intensity I_E is related to the axion phase space density f_a by $I_E = E^3 f_a / h^3 c^2$.

The equation of radiative transport (which follows directly from the Boltzmann equation) governs the evolution of I_E and is given by

$$\frac{1}{c} \frac{\partial I_E}{\partial t} + \hat{n} \cdot \nabla I_E = -\rho \kappa_E (I_E - B_E), \quad (17)$$

where local thermodynamic equilibrium (LTE) is assumed for the nucleon species, B_E is the previously discussed Planck function (for axions), and only axion-absorption and emission processes have been included. Taking the zeroth and first angular moments of this equation, specializing to spherical symmetry, and integrating over axion energy we obtain

$$\frac{d(\rho_a/\rho)}{dt} + p_a \frac{d(1/\rho)}{dt} + \frac{1}{4\pi r^2 \rho} \frac{\partial}{\partial r} (4\pi r^2 F_a) = -c \int \kappa_E (d\rho_a/dE - 4\pi B_E/c) dE, \quad (18)$$

$$F_a = -\frac{c}{3\rho \langle \kappa \rangle_R} \frac{\partial \rho_a}{\partial r} \hat{r}. \quad (19)$$

Here $\rho_a = \int (d\rho_a/dE) dE$ is the axion-energy density, p_a is the axion pressure, F_a is the radial axion-energy flux, and we have used the Eddington approximation, $\rho_a \simeq 3p_a$, which is valid for any nearly isotropic radiation field (i.e., everywhere, except very near the axion sphere).

The general-relativistic version of Eq. (18) was solved by an operator-split method, along with the neutrino-energy transport equations, and the equation of hydrostatic equilibrium. A major simplifying assumption was to take the axions to be in LTE with the matter interior to the axion sphere. In the strongly trapped regime this is a very good approximation. In the transition regime (total ‘‘axion-optical depth’’ $\tau \equiv \int_0^\infty dr/\lambda_a$ between 1 and 100), corresponding to axion masses between 2×10^{-2} eV and about 0.2 eV, this is a marginal approximation as the axion sphere is broad and ill defined. As we discuss in the next Section we were unable to treat the transition region reliably for other reasons too. However, we are confident that the the effect of axion cooling in the transition is so severe that such an axion mass is clearly excluded.

Finally, we mention that we previously tried a less robust approximation to treat axion transport: leakage. In the leakage approximation the effect of axion emission is modeled

by a local heat sink of magnitude $\dot{\epsilon}_a/(1 + k\tau^2)$ where k is a numerical constant of order unity and τ is the total axion optical depth. While leakage schemes have been successfully used in other instances, e.g., neutrino transport,¹⁴ they were not up to the difficult task of treating axion-energy transport. This is in part because the leakage approximation is well suited to the case where the mean-free path and density are constant; in the present circumstance the density varies significantly near the axion sphere (and $\lambda_a \propto \rho^{-2}$). The leakage scheme systematically underestimated the effect of axion cooling.

IV. Results of Numerical Models

For the purpose of this investigation of the trapped regime, we have focused on a single proto neutron-star model, model B from our previous work on the freely streaming regime (Ref. 5, hereafter referred to as BTB). In BTB, we investigated a variety of proto-neutron star models, with different equations of state and different masses, and found substantially the same results for all of the models. We feel confident that we can restrict the present studies of the trapping regime to a single model, model B, the model that best reproduces the neutrino observations of SN 1987A. (Model B has a stiff equation of state and the proto-neutron star mass starts at $1.3 M_\odot$ and increases by accretion to about $1.5 M_\odot$.)

For the most part we will follow the approach of BTB. To briefly remind the reader of the strategy of the previous work, we first computed the neutrino flux from a numerical simulation of the cooling of the nascent neutron star that included freely streaming axion emission. From this flux and the response characteristics of the KII and IMB water Cherenkov detectors we computed the number of $\bar{\nu}_e$ -capture events expected for each detector (N) and the time required for the expected number of events to reach 90% of its asymptotic value ($\Delta t_{90\%}$), again for each detector. In addition, we computed the total energy carried off by axions (E_a) and by neutrinos (E_ν).

Both the energy carried off by neutrinos and the number of capture events were only mildly sensitive to the effects of axion emission; we found that the most sensitive indicator of axion emission was $\Delta t_{90\%}$. As the assumed axion mass was increased to about 10^{-3} eV, the neutrino burst duration dropped precipitously to less than about 1 sec for both detectors, in contrast to the observed burst durations of about 12 sec (KII)¹⁷ and about 6 sec (IMB);¹⁸ see Fig. 3. On this basis, in BTB we concluded that the KII and IMB data excluded an axion more massive than about 10^{-3} eV (at least in the freely streaming regime).

To investigate the trapping regime we used the same general-relativistic code employed in BTB, which is discussed in detail in Refs. 15 and 16. Numerical simulations of the initial cooling phase (first 20 sec after collapse) of a hot neutron star that incorporate the axion diffusion were carried out for axion masses from 0.5 eV to 10 eV. For each model we computed the total energy radiated in axions E_a , the total energy radiated in neutrinos E_ν , and for each detector, the expected number of events N and burst duration $\Delta t_{90\%}$. In addition, at times of 0.01 sec, 0.1 sec, 1.0 sec, 5.0 sec, and 20 sec we computed the

temperature and luminosity of the axion sphere (the bulk of the axion luminosity comes from the axion sphere), red shifted to $r = \infty$. Our results are given in Tables I, II, and III and illustrated in Figs. 1 and 3-6. In addition, both for completeness and comparison, in Figs. 1, 3, and 4 we have shown the results of our previous work for the freely streaming regime.

For model B the total axion-optical depth becomes of order unity for an axion mass of about 0.02 eV, in good agreement with the estimate previously given in Ref. 3. If for the moment we neglect the effect of axion cooling on the structure of the hot neutron star, then the total axion-optical depth scales simply as $\tau \sim (m_a/0.02\text{eV})^2$. From this we see that axions are not strongly trapped (say $\tau \gtrsim 100$) unless $m_a \gtrsim 0.2$ eV. In this awkward transition regime, $m_a \sim 0.02$ eV to 0.2 eV, the axion opacity is significant, and axions are not freely streaming; however, they are not so strongly trapped that there is a well defined axion sphere. Neither treatment is suitable for the transition regime. Moreover, in the transition regime the axion luminosity is near maximum—recall, the simplest expectation is that the axion luminosity peaks for $\tau \sim 1$ —so that the effect of axion cooling is very great.

In attempting to treat the transition regime we discovered another difficulty: During the initial collapse from the white dwarf state ($\rho \sim 5 \times 10^9 \text{ g cm}^{-3}$ and $T \sim 0.5 \text{ MeV}$) and just before the proto neutron star state is reached, the total axion optical depth will reach unity and the axion luminosity will be very large ($10^{55} \text{ ergs sec}^{-1}$ in one case we studied). So large in fact that the initial model we assume for the nascent neutron star is not self consistent as the collapsing core will certainly be affected significantly by axion emission during the collapse. In order to self consistently consider an axion mass of between 0.02 eV and 0.2 eV one would have to take into account the effect of axion emission on the collapse phase. For these reasons we decided that the transition region was beyond the scope of the present investigation, and only considered axion masses greater than 0.5 eV, for which $\tau \gtrsim 1000$ and the effect of axion emission on the collapse and initial state of the neutron star should not be very large. We would argue strongly that the effect of axion cooling for axion masses between 0.01 eV and 0.5 eV is so severe that an axion of this mass is most certainly precluded. For such masses there is every reason to expect that the energy carried away by axions is greater than that for a mass of 0.5 eV, and therefore that the burst duration should be shorter. We should emphasize that because of the dependence of the axion-mean-free path on density and temperature, for any axion mass between about 0.03 eV and 30 eV axions will, at the onset of collapse, be freely streaming and then, only late in the collapse, will they become trapped. As they become trapped their luminosity will be achieve its maximum value. Thus we expect that axions of mass greater than about 0.02 eV will affect the collapse and the initial state of the proto neutron star.

Because axion emission during the initial collapse phase can be significant—and we do not take it into account—we decided that it was important to check the consistency of our treatment. Our chief concern is the fact the the initial state we assume for the proto

neutron star is not quite “relaxed.” That is, because energy transport by axions was not included during the collapse phase, the temperature gradient and lepton number gradient are not quite what they should be; had we included the effect of axion cooling during the collapse phase, the initial proto neutron star would be relaxed. To gauge the importance of the “mismatch” in initial conditions, in Table I we show the energy radiated in axions before and after the proto neutron state relaxes. For an axion mass of 0.5 eV these energies are almost equal; for a mass of 1 eV the energy radiated before relaxation is only about 1/3 of the total energy radiated; and for a mass of about 3 eV it is only about 25%. We should emphasize that the mismatch in the initial state only leads to an uncertainty in the energy radiated while the neutron star is relaxing to equilibrium. Owing to this fact we estimate an uncertainty in the predicted number of neutrino events of about $\pm 1/2$ event which, for our purposes is not significant.

The behavior of our best barometer for axion emission—the burst duration $\Delta t_{90\%}$ —is shown in Fig. 3 for axion masses from 10^{-4} eV to 10 eV, spanning both the freely streaming and trapping regimes. One can clearly see the effect of axion emission on the neutrino burst: As the axion mass is increased to about 10^{-3} eV the burst duration drops precipitously due to the effect of axion emission; at a mass of about 10^{-2} eV, where trapping begins, the burst duration is less than 1 sec for both KII and IMB. For masses between 0.01 eV and 0.5 eV we strongly suspect that the burst duration remains shorter than about 1 sec, but as discussed above we have been unable to reliably treat this regime. At a mass of 0.5 eV the IMB burst duration is still less than about 0.5 sec and the KII burst duration is less than 2 sec. As the axion mass is increased beyond 0.5 eV trapping reduces the effect of axion emission, and $\Delta t_{90\%}$ increases. For an axion mass of 2 eV the predicted burst duration for KII is about 5 sec, about half of the predicted duration in the absence of axion emission. For an axion mass of about 4 eV the IMB burst duration has increased to 2 sec, about half of the predicted burst duration in the absence of axion emission. On this basis we would set the upper boundary of the excluded mass interval to be about 3 eV.

The reader is reminded that the physical origin of the precipitous drop in burst duration, first found in BTB, can be traced to the fact that there are two distinct phases of neutrino emission. The first phase, lasting of order 1 sec, is powered by the heat in the outer mantle and residual accretion; the second phase, lasting of order many seconds, is powered by the outward diffusion of the heat trapped in the inner core. The first phase is rapid because the timescales for neutrino diffusion out of the low density outer mantle and for residual accretion are both short ($\lesssim 1$ sec). The second phase lasts much longer because the timescale for diffusion of neutrinos from the inner core is long, of order many seconds. Axion emission tends to deplete the heat trapped in the inner core that powers the second phase of neutrino emission by providing another means of transporting heat out of the inner core. By so doing, axion emission can drastically shorten the duration of the neutrino burst.

As in the freely streaming regime, the number of capture events (see Fig. 5) and the

energy carried off by neutrinos (see Fig. 1) are much less sensitive indicators of axion emission: At a mass of about 10^{-2} eV the expected number of events falls by less than a factor of 2, and, at most, axions carry away as much energy as the neutrinos do. This is simple to understand: Axion emission does not directly suppress neutrino emission; rather, axions tap the same source of energy as do neutrinos, and thus, axion cooling serves mainly to shorten the cooling time.

There is one new interesting twist in the trapping regime: The number of events expected for the IMB detector *rises* above its value for no axion cooling at an axion mass of 0.5 eV, before relaxing to its no axion cooling value for large axion mass. This odd phenomenon has a simple explanation: For axion masses around 0.5 eV, axions are very efficient in transporting energy from deep in the core out to the neutrino sphere, thereby heating the neutrino sphere. Because of the high energy threshold of the IMB detector, the number of events expected at IMB is very sensitive to the temperature of the neutrino sphere.

The total energy carried away by axions is shown in Fig. 1 and Table I. In the regimes where axions are a minor heat sink, axion masses much smaller than 10^{-2} eV or much greater than 1 eV, one can, for purposes of understanding how E_a scales, ignore the back reaction of axions on the cooling of the neutron star. Doing so, in the low mass regime one expects the energy carried off by axions should vary as m_a^2 since the axion luminosity is proportional to $\dot{\epsilon}_a$ which varies as m_a^2 . In the high mass regime, the situation is more complicated because of axion trapping. However, one expects the axion luminosity to vary as the temperature of the axion sphere to the fourth power, and in Ref. 3 it was estimated that the temperature of the axion sphere should vary as $m_a^{-4/11}$; this implies that the energy carried off by axions should vary as $m_a^{-16/11}$ in the large mass limit. Both of these scalings are roughly consistent with our numerical results for the temperature of the axion sphere and the energy carried away by axions.

It may be of some interest to know the average energy of the axions emitted by a nascent neutron star in the trapping regime, e.g., if one envisions nascent neutron stars as an intense source of axions that might be detected by other means.¹⁹ In Table II and Fig. 5 we have shown the temperature of the axion sphere at times of 0.01 sec, 0.1 sec, 1.0 sec, and 20 sec. (The axion sphere is the surface beyond which the number of axion-mean-free paths, or "optical depth," equals 2/3; i.e., $\int_{R_a}^{\infty} \rho \langle \kappa \rangle_R dr = \int_{R_a}^{\infty} dr / \lambda_a = 2/3$.) The temperature has been red shifted to $r = \infty$: $T_{\infty} = T_a / (1 + z)$ where $(1 + z)$ is the gravitational red shift from the axion sphere to infinity. (The total energies carried off by axions and neutrinos discussed earlier were red shifted in the same way.) The average axion energy is related to the temperature of the axion sphere by $\langle E_a \rangle = 2.7 T_a / (1 + z)$. One can see that the temperature of the axion sphere drops roughly as a power law, $T_{\infty} \propto t^{-1/4}$, from which it follows that the energy radiated in axions per logarithmic interval of time is roughly constant. In Fig. 6 we display the axion luminosity from the axion sphere at the same times; very roughly, \mathcal{L}_a decreases as t^{-1} , as one would expect since $\mathcal{L}_a \propto T_a^4$ and

$$T_a \propto t^{-1/4}.$$

Next, we briefly comment upon the inclusion of the pion-propagator correction factor $R(\alpha, T)$. In general, its effect upon our results was small (typically 10% to 20%) and would not have significantly affected any of our conclusions (had we not included it). As expected, the effect of including this correction was most significant for large axion masses, for which the temperature of the axion sphere is the smallest (recall that $T_a \propto m_a^{-4/11}$). Based upon the very small effect of including this correction, we feel confident that not including the pion-propagator in our previous work⁵ was a well justified approximation. In particular, we re-ran model B for freely streaming axions of mass 10^{-2} eV, including the pion-propagator correction, and the results changed insignificantly.

Finally, we wish to illustrate the richness involved in adding the effect of axions to the initial cooling of a hot neutron star. For comparison, we have run some initial cooling models without axion cooling, but with the addition of extra light (mass $\ll 10$ MeV) neutrino species. In Figs. 7 and 8 we show the predicted number of events and burst duration $\Delta t_{90\%}$ for the KII and IMB detectors as a function of the number of neutrino flavors, $N_\nu = 3$ to 11. (The additional neutrino species, like the μ and τ neutrinos were assumed to couple only through the neutral current interaction.) As can be seen from these Figures, the effect of additional neutrino species has a much less dramatic effect: The number of events and burst duration decrease slowly with N_ν . The reason is simple. Since all neutrino species couple with weak interaction strength, their effect on transport of heat from the inner core is minimal. (Very roughly, the effect of additional neutrino species on neutrino energy transport is to increase the effective neutrino coupling strength by a factor of $(N_\nu/3)^{1/2}$.) The additional species serve mainly to dilute the energy carried off by electron antineutrinos, because the energy released from the gravitational collapse of the core must be shared among more degrees of freedom. In contrast, as the axion mass is varied the coupling strength varies (as m_a). By varying m_a from 10^{-4} eV to 10 eV, one explores a range of qualitatively different regimes, from freely streaming to strongly trapped, and the effect on the cooling of the newly born neutron star is much more dramatic. While one can exclude an axion in the mass range of 10^{-3} eV to about 3 eV based upon the KII and IMB observations, based upon the same observations one would be hard pressed to exclude as many as 5 additional neutrino species. Of course, the existence of more than 3 light neutrino species is now firmly excluded by the precise measurements of the width of the Z^0 boson made by the SLC experiment at SLAC and the ALEPH, DELPHI, L3, and OPAL experiments at LEP.¹⁹

V. Concluding Remarks

The existence of an axion of mass in the range 10^{-3} eV to about 10 eV would have had a significant effect upon the cooling of the nascent neutron star associated with SN 1987A (and upon other newly born neutron stars). For such a mass, axions would carry away a significant fraction of the energy and would significantly accelerate the cooling

process. We have now investigated in detail the effect of axion cooling both in the freely streaming regime ($m_a \lesssim 10^{-2}$ eV) and in the trapping regime ($m_a \gtrsim 10^{-2}$ eV). Based upon the duration of the expected neutrino bursts calculated in our axion-cooled models, an axion mass in the interval 10^{-3} eV to 3 eV can be excluded. The upper mass boundary is very close to the original estimate made in Ref. 3. Therefore, the axion mass window around a few eV remains the same, from about 3 eV to 5 eV (hadronic axions only). The entire window was explored by a search for the decays of relic cosmological axions that was carried out at Kitt Peak this year.⁶ If that search is unsuccessful, it will close the multi-eV axion-mass window. The multi-eV window is also accessible through an experiment that has been proposed to search for axions emitted by the Sun.⁷ It is also possible that this mass region could be explored if a supernova explosion occurred within our own galaxy, e.g., by more closely examining the neutrino signal (provided that many more events are detected) or by other means such as gamma-ray observations.²⁰

As we emphasized earlier in this paper and in BTB, our results, which are expressed in terms of the axion mass, actually depend upon the values of the axion-nucleon couplings; for definiteness we have assumed that $c_n = c_p = \frac{1}{2}$ where $g_{an} = c_n m_N / (f_a / N)$ and $g_{ap} = c_p m_N / (f_a / N)$. The dimensionless axion-nucleon couplings c_n and c_p depend upon the PQ charges of the quark species and the quark-distribution functions; the couplings are discussed in some detail in Refs. 21. Both mass boundaries for the excluded mass region scale with the inverse of the axion-nucleon couplings; that is, doubling c_n and c_p would decrease both the upper and lower mass boundaries by a factor of two. (Of course, the re-scaling of the boundaries of the excluded region is more difficult if c_n and c_p do not change in the same way; however, one could probably still estimate the change.)

Finally, we should mention the uncertainties inherent in our axion mass constraint. To begin with, there are the uncertainties associated with our numerical cooling models—equation of state, neutron star mass, amount of residual accretion, the diffusion approximation used for axion transport, and our exclusion criterion for the duration of the neutrino burst. While these uncertainties could amount to a factor of two or so in the mass boundary, additional uncertainty beyond that does not seem likely. The uncertainty in the axion-emission rate and opacity are a different matter. Deep in the core of the nascent neutron star the densities certainly reach several times that of nuclear matter; there may be high-density effects, nuclear many-body effects—or even an exotic form of matter at the core, e.g., quark matter or a pion condensate—that could significantly affect the axion emission rate or opacity. The high-density effects have discussed in Ref. 11 and do not seem likely to affect either the axion luminosity or opacity significantly. In any case, the uncertainties associated with the high densities at the core of the neutron star would probably only affect the low mass boundary, as only in the freely streaming regime does most of the axion luminosity come from the core. In the trapping regime, most of the axion luminosity comes from the axion sphere, which around the upper mass boundary is characterized by rather modest temperatures, around 10 MeV, and densities, around 10^{13}

g cm^{-3}).

To be more specific, it was pointed out in Ref. 11 that axion emission from the core could be strongly suppressed if the core was quark/gluon matter rather than hot nuclear matter, since the axion-quark coupling is significantly smaller than the axion-nucleon coupling. Very recently, Ellis and Salati²² have considered this effect quantitatively and concluded that the existence of a quark/gluon matter core would significantly raise the lower boundary of the excluded region. Based upon the present work, we would argue that the lower boundary would not be raised to more than about 0.01 eV, the mass where trapping sets in. For an axion mass up to about 0.5 eV, the axion luminosity during the initial collapse phase (before the quark/gluon core can form) is prohibitively large. Furthermore, in the trapping regime, axions are in thermal equilibrium from the axion sphere (densities around $10^{13} \text{ g cm}^{-3}$) inward to the boundary of the quark/gluon core; thus, the absence of a thermal bath of axions deep in the quark/gluon core should not significantly affect the axion luminosity, which arises primarily from axion production near the axion sphere. (Of course, we are simplifying matters; the presence of a quark/gluon core would also greatly lessen the effect of axion energy transport from the core outward—and in some cases inward. Firm conclusions await a detailed treatment of proto neutron star cooling models with a quark/gluon core.)

Almost since its conception, it has been realized that the axion could significantly affect the cooling of stars of all kinds. Because the evolutionary timescales for most stars are measured in millions, if not billions, of years, the astrophysical arguments based upon stellar evolution that have been used to constrain the axion mass have necessarily been indirect.² The lone exception is SN 1987A; here the 19 neutrino events detected by KII and IMB provide the complete cooling history of the newly born neutron star. Based upon that cooling record an axion mass in the range 10^{-3} eV to 3 eV is excluded. Not only is this constraint the most stringent astrophysical constraint to the axion mass, but the directness of the argument is most pleasing.

Acknowledgments

We thank D. Seckel for his critical remarks. This work was supported in part by the DOE (at Chicago and Fermilab), the NASA through NAGW-1340 (at Fermilab) and through MTR's GSRP (at Chicago), and by the NSF through Grants No. AST 87-14176 and 89-14346 (at Arizona).

References

1. R.D. Peccei and H.R. Quinn, *Phys. Rev. Lett.* **38**, 1440 (1977); F. Wilczek, *Phys. Rev. Lett.* **40**, 279 (1978); S. Weinberg, *Phys. Rev. Lett.* **48**, 223 (1978). The "invisible axion" is of two generic types: DFS, first discussed by M. Dine, W. Fischler, and M. Srednicki, *Phys. Lett. B* **104**, 199 (1981), and A. Zhitnitsky, *Yad. Fiz.* **31**,

- 497 (1980) [*Sov. J. Nucl. Phys.* **31**, 260 (1980)]; and hadronic, first discussed by J.-E. Kim, *Phys. Rev. Lett.* **43**, 103 (1979), and M. Shifman, A. Vainshtein, and V. Zakharov, *Nucl. Phys.* **B166**, 493 (1980). For a recent review of the axion see R.D. Peccei, in *CP Violation*, edited by C. Jarlskog (WSPC, Singapore, 1989).
2. See, e.g., M.S. Turner, in *Proc. of the Workshop on Cosmic Axions*, edited by C. Jones and A. Melissinos (WSPC, Singapore, 1990), and *Phys. Rept.*, in press (1990); or G.G. Raffelt, *Phys. Rept.*, in press (1991).
 3. M.S. Turner, *Phys. Rev. Lett.* **60**, 1797 (1988).
 4. N. Iwamoto, *Phys. Rev. Lett.* **53**, 1198 (1984); A. Pantziris and K. Kang, *Phys. Rev. D* **33**, 3509 (1986); J.E. Ellis and K.A. Olive, *Phys. Lett. B* **193**, 525 (1987); R. Mayle, et al., *Phys. Lett. B* **203**, 188 (1988); *ibid* **219B**, 515 (1989); G.G. Raffelt and D. Seckel, *Phys. Rev. Lett.* **60**, 1793 (1988); M.S. Turner, *ibid* **60**, 1797 (1988); A. Burrows, M.S. Turner and R.P. Brinkmann, *Phys. Rev. D* **39**, 1020 (1989); R.P. Brinkmann and M.S. Turner, *Phys. Rev. D* **38**, 2338 (1988); M.S. Turner, H.-S. Kang, and G. Steigman, *Phys. Rev. D* **40**, 299 (1989); K. Choi, K. Kang, and J.-E. Kim, *Phys. Rev. Lett.* **62**, 849 (1989); N. Iwamoto, *Phys. Rev. D* **39**, 2120 (1989); M. Carena and R.D. Peccei, *Phys. Rev. D* **40**, 652 (1989); T. Hatsuda and M. Yoshimura, *Phys. Lett. B* **203**, 469 (1988); T.E.O. Ericson and J.-F. Mathiot, *Phys. Lett. B* **219**, 515 (1989); N. Ishizuka and M. Yoshimura, Tohoku Univ. preprint TU-349 (1989).
 5. A. Burrows, M.S. Turner, and R.P. Brinkmann, *Phys. Rev. D* **39**, 1020 (1989).
 6. T. Kephart and T. Weiler, *Phys. Rev. Lett.* **58**, 171 (1987); M.S. Turner, *Phys. Rev. Lett.* **59**, 2489 (1987); M. Bershadsky, M.T. Ressell, and M.S. Turner, Kitt Peak observing run, 23-25 May 1990, and manuscript in preparation (1990).
 7. K. van Bibber, P.M. Mc Intyre, D.E. Morris, and G.G. Raffelt, *Phys. Rev. D* **39**, 2089 (1989).
 8. See, e.g., D. Kaplan, *Nucl. Phys.* **B260**, 215 (1985); M. Srednicki, *Nucl. Phys.* **B260**, 689 (1985); P. Sikivie, in *Cosmology and Particle Physics*, edited by E. Alvarez et al. (WSPC, Singapore, 1986); R. Mayle, et al., *Phys. Lett. B* **219**, 515 (1989); or Ref. 3. The conventions and notation here follow Ref. 3.
 9. R.P. Brinkmann and M.S. Turner, *Phys. Rev. D* **38**, 2338 (1988); in the degenerate regime the matrix element and phase-space have also been evaluated by N. Iwamoto, *Phys. Rev. Lett.* **53**, 1198 (1984). The fully relativistic matrix element and phase-space integrations have been carried out by M.S. Turner, H.-S. Kang, and G. Steigman, *Phys. Rev. D* **40**, 299 (1989), and by N. Ishizuka and M. Yoshimura, Tohoku Univ. preprint TU-349 (1989).
 10. N. Ishizuka and M. Yoshimura, Tohoku Univ. preprint TU-349 (1989). Since they calculate λ_a in the completely degenerate limit, their work is complementary to the present work and not applicable for the initial stages of cooling since the conditions are nondegenerate.

11. M.S. Turner, H. Kang, and G. Steigman, *Phys. Rev. D* **40**, 299 (1989); also see, Ishizuka and Yoshimura in Ref. 10.
12. I.S. Gradshteyn and I.M. Ryzhik, *Table of Integrals, Series, and Products* (Academic Press, London, 1980), p. 319.
13. See, e.g., G.W. Collins, *The Fundamentals of Stellar Atmospheres* (W.H. Freeman & Co., New York, 1989), pp. 227-251, 303-307; S.L. Shapiro and S.A. Teukolsky, *Black Holes, White Dwarfs, and Neutron Stars* (J. Wiley & Sons, New York, 1983); D. Mihalas, *Stellar Atmospheres* (W.H. Freeman, San Francisco, 1970), pp. 1-41; D. Mihalas and B.W. Mihalas, *Foundations of Radiation Hydrodynamics* (Oxford Univ. Press, New York, 1984).
14. More precisely, the constant k is a geometric factor. Axions emitted by a shell at radius r diffuse in all directions—from radially outward where the opacity “seen” by axions is only $\int_r^\infty dr/\lambda_a$ to radially inward where the opacity “seen” by axions is $2 \int_r^\infty dr/\lambda_a + \int_r^\infty dr/\lambda_a$. By replacing τ_D/τ_a by $k[\int_0^\infty dr/\lambda_a]^2$, k takes into account the average opacity seen over all directions. For a constant density model and the fundamental mode of diffusion one can show that $k = 3/\pi^2$; see, e.g., G.B. Rybicki and A.P. Lightman, *Radiative Processes in Astrophysics* (J. Wiley & Sons, New York, 1979). In many circumstances the value of k that best reproduces the results of a proper treatment of energy transport does not differ much from $k = 0.3$. In the context of neutrino transport in neutron stars the leakage approximation scheme has been studied extensively by K. Van Riper and J.M. Lattimer, *Astrophys. J.* **249**, 270 (1981). One might want to compare the results of neutrino transport in neutron stars using a leakage scheme (A. Burrows and J.M. Lattimer, *Astrophys. J.* **299**, L19 (1985)) with those using full neutrino transport (S.W. Bruenn, *Astrophys. J. Suppl.* **58**, 771 (1986)). Unfortunately, in the present circumstance the strong dependence of the axion opacity upon density and the rapid variation of density near the axion sphere, precluded the use of the more manageable leakage approximation.
15. A. Burrows and J.M. Lattimer, *Astrophys. J.* **307**, 178 (1986).
16. A. Burrows, *Astrophys. J.* **334**, 891 (1988).
17. R.M. Bionta, et al., *Phys. Rev. Lett.* **58**, 1494 (1987).
18. K. Hirata, et al., *Phys. Rev. Lett.* **58**, 1490 (1987).
19. G.S. Abrams et al., *Phys. Rev. Lett.* **63**, 2173 (1989) (SLC); B. Adeva et al., *Phys. Lett. B* **231**, 509 (1989) (L3); D. Decamp et al., *Phys. Lett. B* **231**, 519 (1989) (ALEPH); M.Z. Akrawy et al., *Phys. Lett. B* **231**, 530 (1989) (OPAL); P. Aarnio et al., *Phys. Lett. B* **231**, 539 (1989) (DELPHI).
20. E.W. Kolb and M.S. Turner, *Phys. Rev. Lett.* **62**, 509 (1989). Very recently, J. Engel et al. [Bartol Research Institute preprint BA-90-11 (1990)] have considered the possibility that multi-eV mass axions radiated from SN 1987A would have induced nuclear transitions in the oxygen in the KII detector that should have led to tens of events for an axion of mass greater than about 6 eV.

21. M.S. Turner, *Phys. Rept.*, in press (1990); G.G. Raffelt, *Phys. Rept.*, in press (1991);
Ref. 3; R. Mayle, et al., *Phys. Lett. B* **219**, 515 (1989).
22. J. Ellis and P. Salati, CERN preprint (1990).

FIGURE CAPTIONS

- Fig. 1. Total energy carried off from SN 1987A by axions (solid curve) and neutrinos (broken curve) as a function of axion mass. The results for $m_a \leq 10^{-2}$ eV were taken from our previous work⁵ (model B). The results for $m_a \geq 0.5$ eV are from the present work. As explained in the text for technical reasons we were unable to consider axion mass between 0.03 eV and 0.5 eV; however, we do not expect any surprises in this mass interval. In agreement with simple arguments, the energy carried off by axions scales very roughly as m_a^2 for small axion masses and as $m_a^{-1.6}$ for large axion masses.
- Fig. 2. The pion-propagator reduction factor, $R(\alpha, T)$, as a function of temperature for $\alpha = E_a/T = 1, 4, 7,$ and 10 . The pion-propagator reduction factor is the factor by which the pion propagators in the matrix element for nucleon-nucleon, axion bremsstrahlung reduce both the axion-emission rate and opacity relative to the approximation where the pion-propagator factors are ignored, cf. Eq. (16).
- Fig. 3. The expected neutrino-burst duration, $\Delta t_{90\%}$, in the KII and IMB detectors for axion-cooled nascent neutron star models as a function of axion mass. The results for $m_a \leq 10^{-2}$ eV were taken from our previous work⁵ (model B). The results for $m_a \geq 0.5$ eV are from the present work. The quantity $\Delta t_{90\%}$ is the time required for the expected number of neutrino events to achieve 90% of its asymptotic value. As explained in the text for technical reasons we were unable to consider axion mass between 0.03 eV and 0.5 eV; however, we expect that the burst duration is very short in this mass interval. Based upon the expected duration of the neutrino burst, axion masses in the interval 10^{-3} eV to 3 eV are excluded by the KII and IMB data. Note that the burst duration in both detectors is reduced by about the same factor.
- Fig. 4. The expected number of neutrino-capture events for the KII and IMB detectors for our axion-cooled neutron star models as a function of axion mass. The results for $m_a \leq 10^{-2}$ eV were taken from our previous work⁵ (model B). The results for $m_a \geq 0.5$ eV are from the present work. As explained in the text for technical reasons we were unable to consider axion mass between 0.03 eV and 0.5 eV. The intriguing increase in the number of events predicted for IMB for axion masses around a few 0.1 eV is due to the fact that axion energy transport heats the neutrino sphere, and because of its high threshold the IMB detector is very sensitive to the temperature of the neutrino sphere. As described in Section IV, the expected number of events is relatively insensitive to the effect of axion cooling.
- Fig. 5. The temperature of the axion sphere (red shifted to $r = \infty$) at times of 0.01 sec, 0.1 sec, 1.0 sec, 5.0 sec, and 20. sec.
- Fig. 6. The axion luminosity from the axion sphere (red shifted to $r = \infty$) at times of 0.01 sec, 0.1 sec, 1.0 sec, 5.0 sec, and 20. sec.
- Fig. 7. Predicted burst duration $\Delta t_{90\%}$ as a function of the number of light (mass $\ll 10$ MeV)

neutrino flavors. These models do not incorporate axion cooling and are shown only to compare the effect of additional neutrino flavors with the effect of axion cooling.

Fig. 8. Predicted number of events as a function of the number of neutrino flavors. These models do not incorporate axion cooling.

Table I. Summary of axion-cooled nascent neutron star models for axion masses from 0.5 eV to 10 eV. All models were run for the first 20 seconds after collapse.

Axion mass (eV)	Number of events		Energy (10^{51} ergs)			$\Delta t_{90\%}$ (sec)	
	KII	IMB	Axions (before)	Axions (after)	$\nu\bar{\nu}$	KII	IMB
0.5	9.0	8.7	40	53.7	147.5	1.7	0.4
1.0	9.1	7.4	21	44.9	160.3	3.5	0.6
2.0	9.9	7.0	12	28.2	181.3	5.0	1.0
3.0	10.2	6.5	7	19.8	193.0	6.8	1.6
4.0	10.2	6.0	5	15.5	198.0	7.5	2.2
5.0	10.2	5.8	3	12.4	202.0	8.0	2.7
7.0	10.2	5.3	2	8.6	207.4	8.7	3.6
10.0	10.3	5.1	1	5.9	213.3	9.1	4.1

Table II. Temperature of the axion sphere, red shifted to $r = \infty$ and given in MeV, as a function of time.

m_a (eV)	10 ms	100 ms	1.0 sec	5.0 sec	20.0 sec
0.5	15.1	9.7	5.6	3.9	1.7
1.0	13.2	9.5	4.6	3.6	2.0
2.0	11.3	7.2	4.2	3.2	1.95
3.0	10.2	6.0	3.8	2.8	1.7
4.0	9.6	5.7	3.8	2.7	1.7
5.0	9.4	4.9	3.5	2.6	1.6
7.0	8.9	4.4	3.0	2.3	1.4
10.0	7.9	3.7	2.6	1.9	1.2

Table III. Axion luminosity from the axion sphere, red shifted to $r = \infty$ and given in 10^{51} ergs sec^{-1} , as a function of time.

m_a (eV)	10 ms	100 ms	1.0 sec	5.0 sec	20.0 sec
0.5	490	65	6.6	1.5	0.058
1.0	370	71	33	1.2	0.1
2.0	215	28	2.4	0.73	0.095
3.0	184	15	1.75	0.45	0.06
4.0	157	14	1.67	0.40	0.055
5.0	160	8.3	1.29	0.30	0.045
7.0	150	5.85	0.72	0.19	0.026
10.0	124	3.0	0.46	0.10	0.012

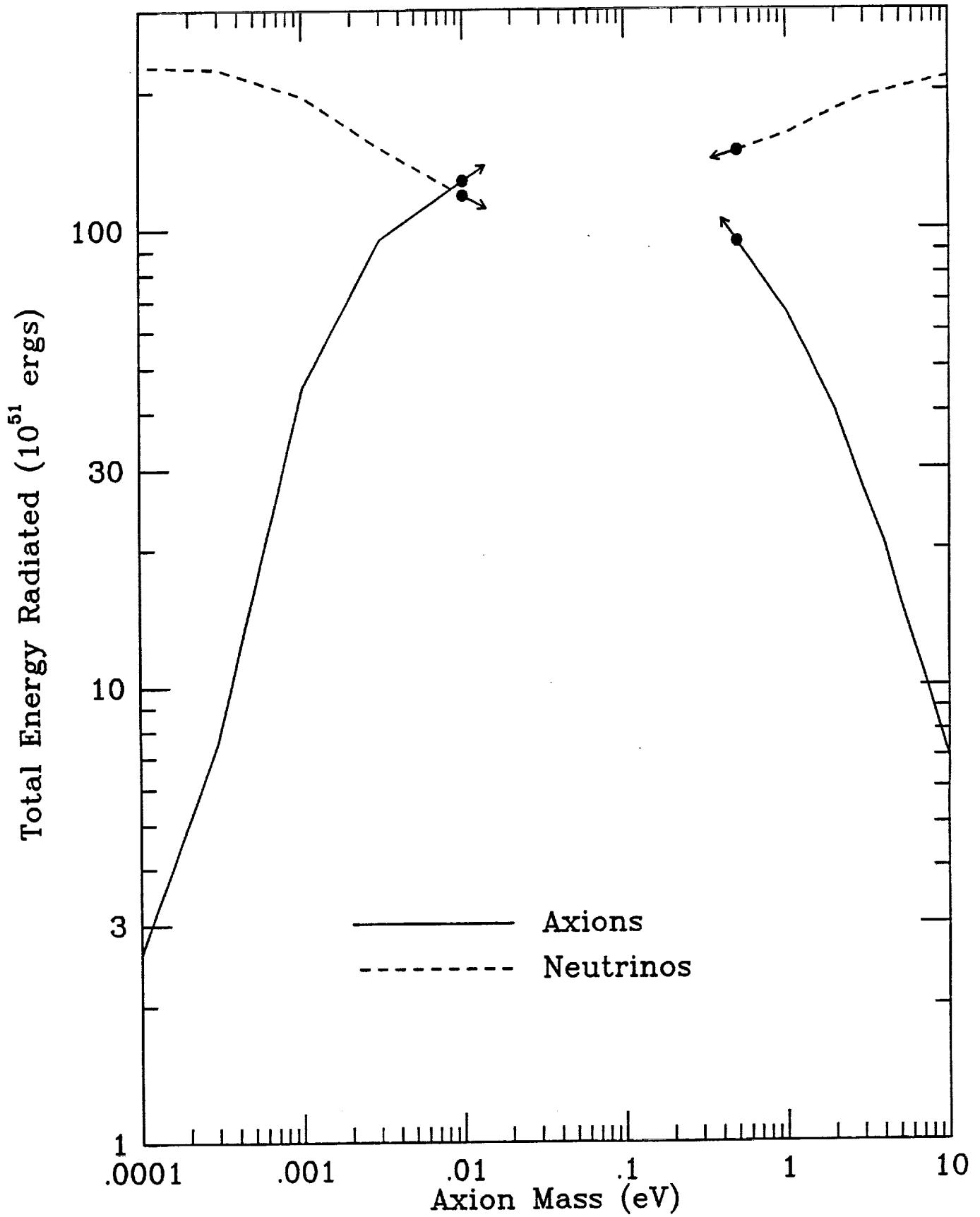


Figure 1

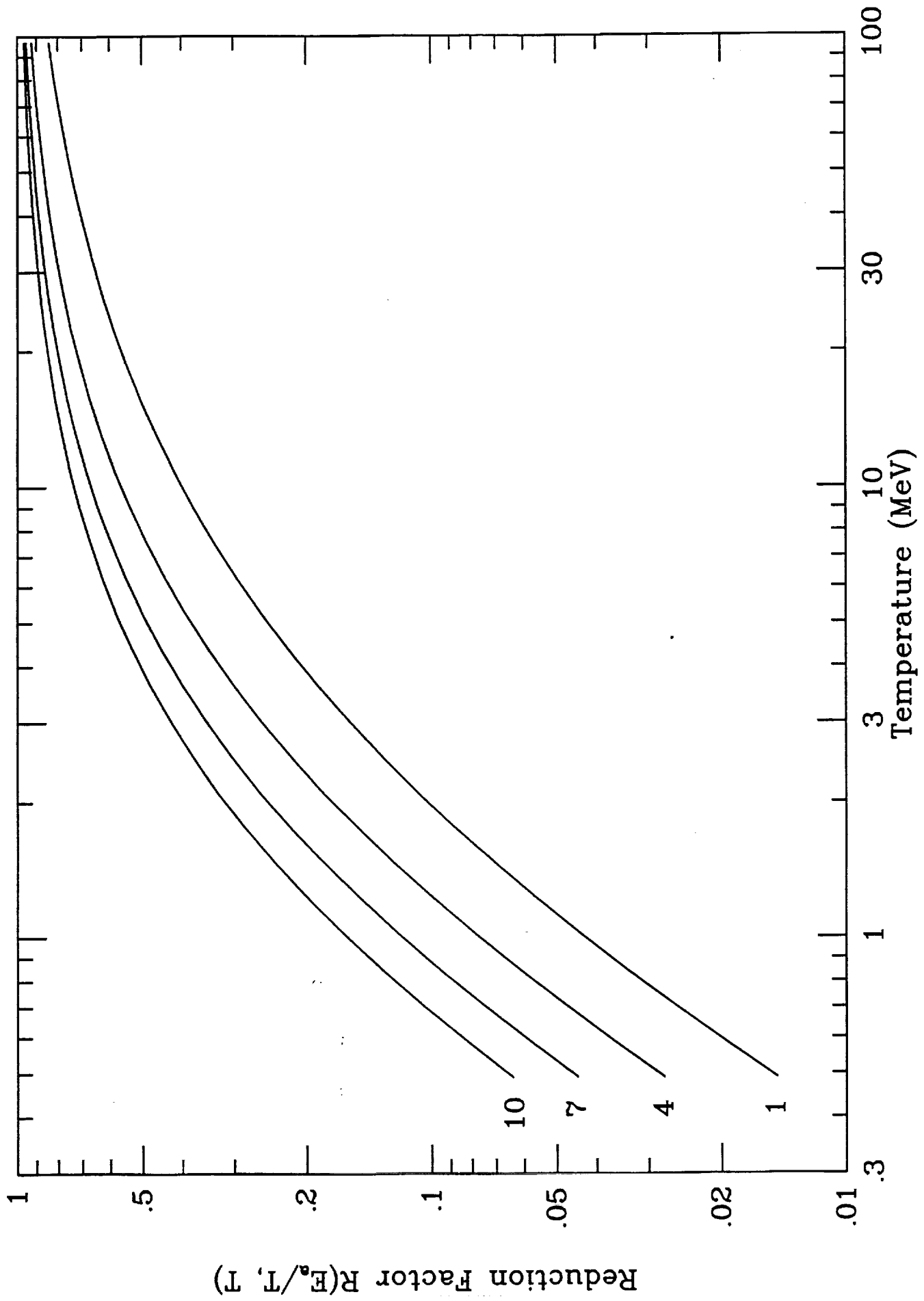


Figure 2

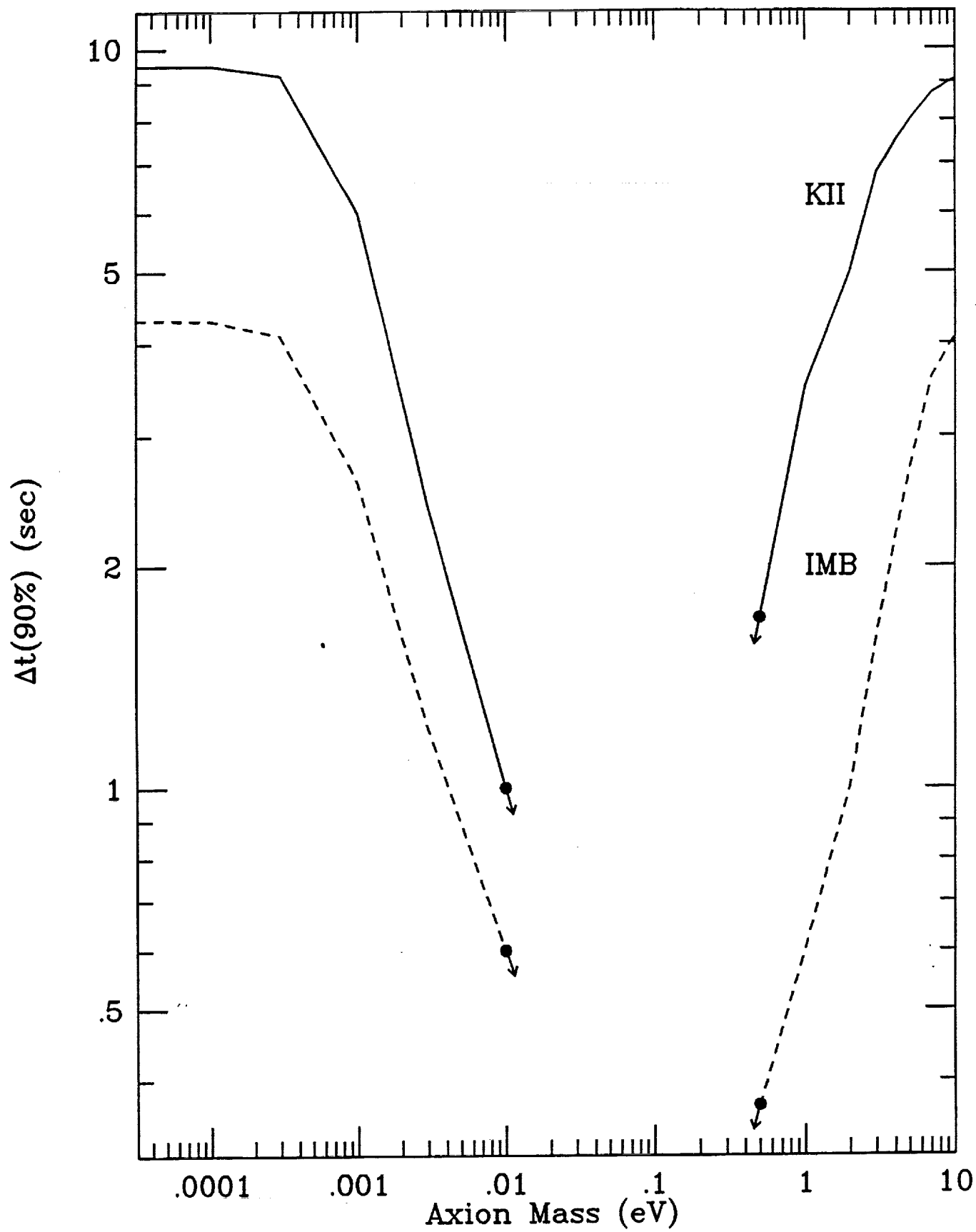


Figure 3

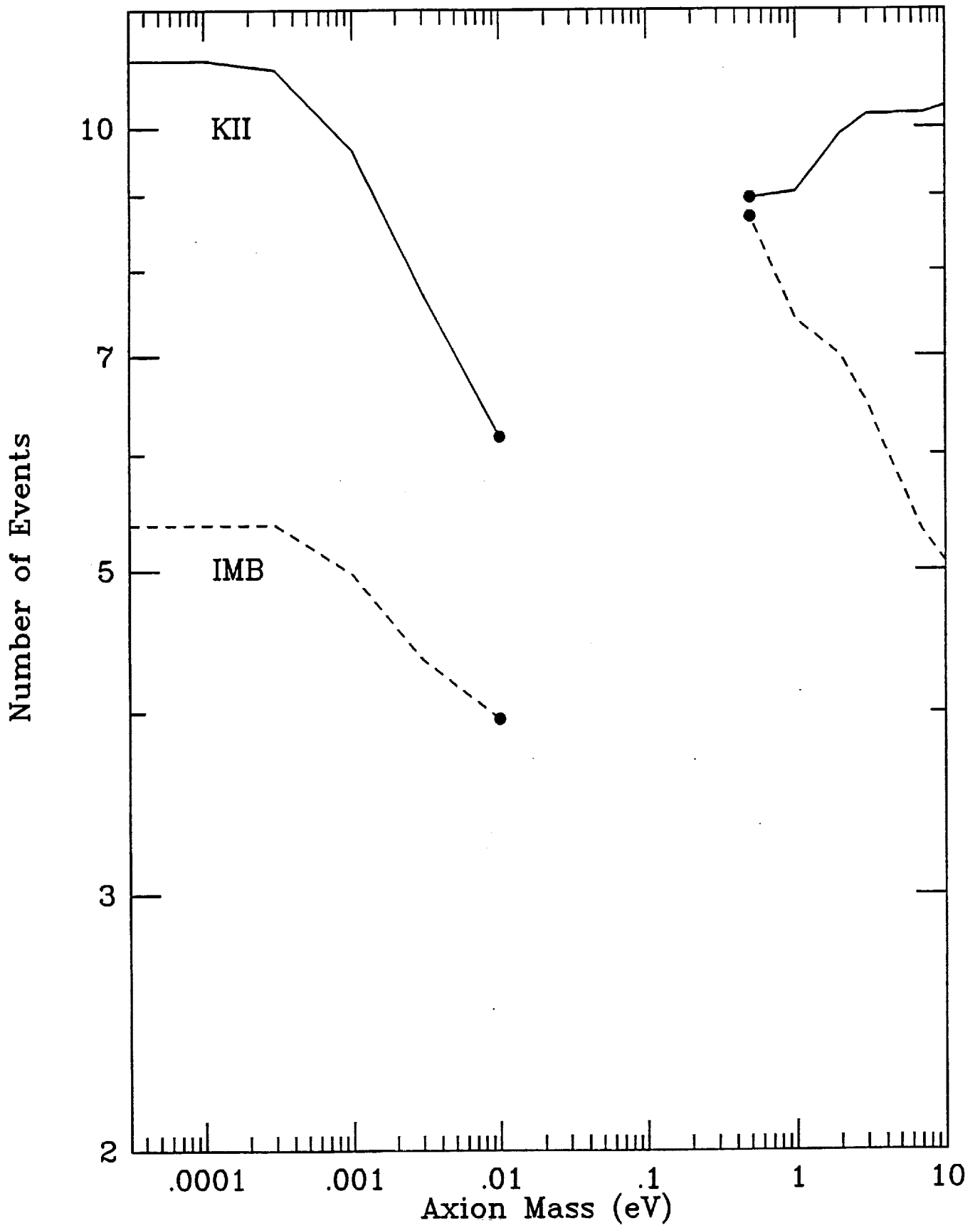


Figure 4

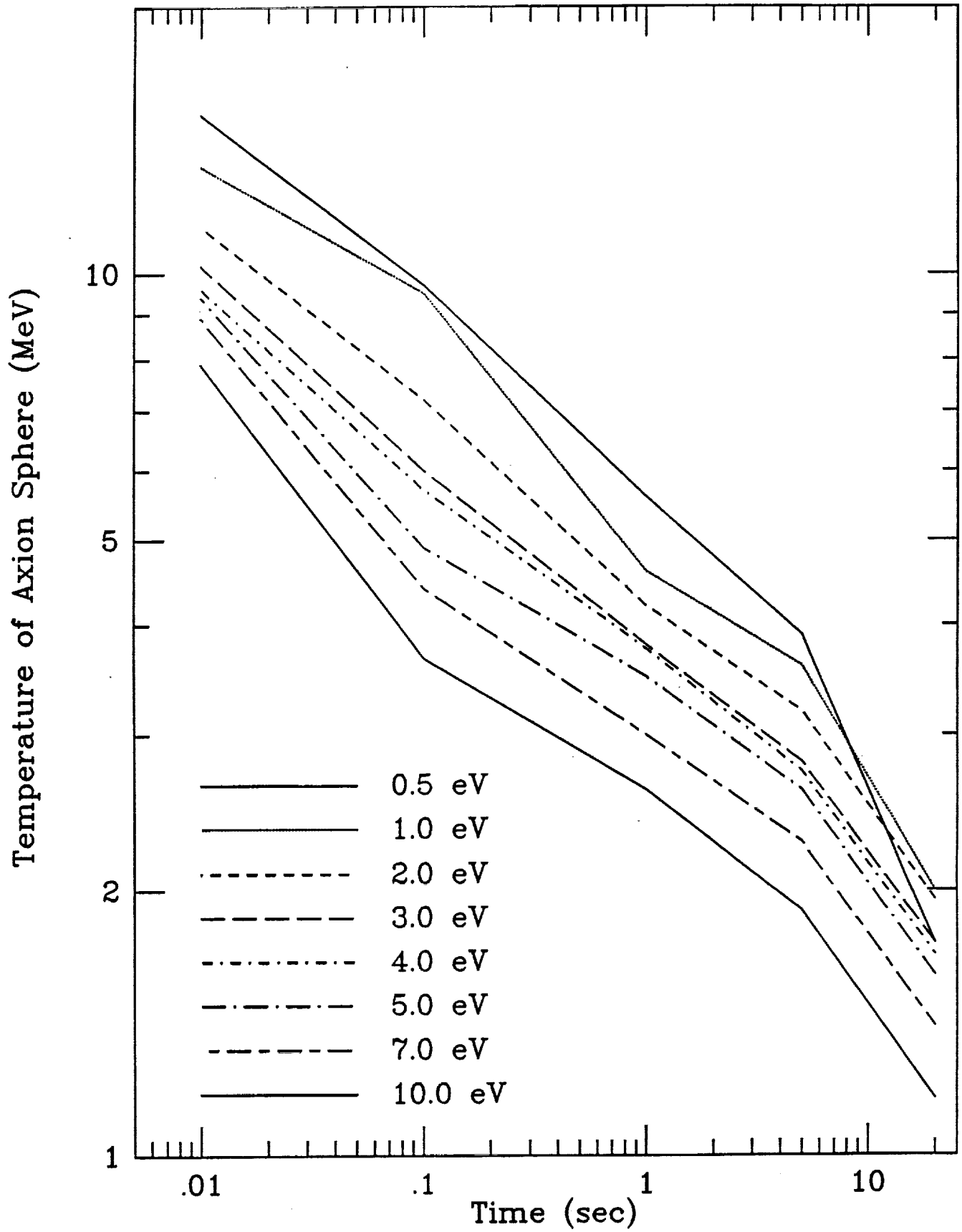


Figure 5

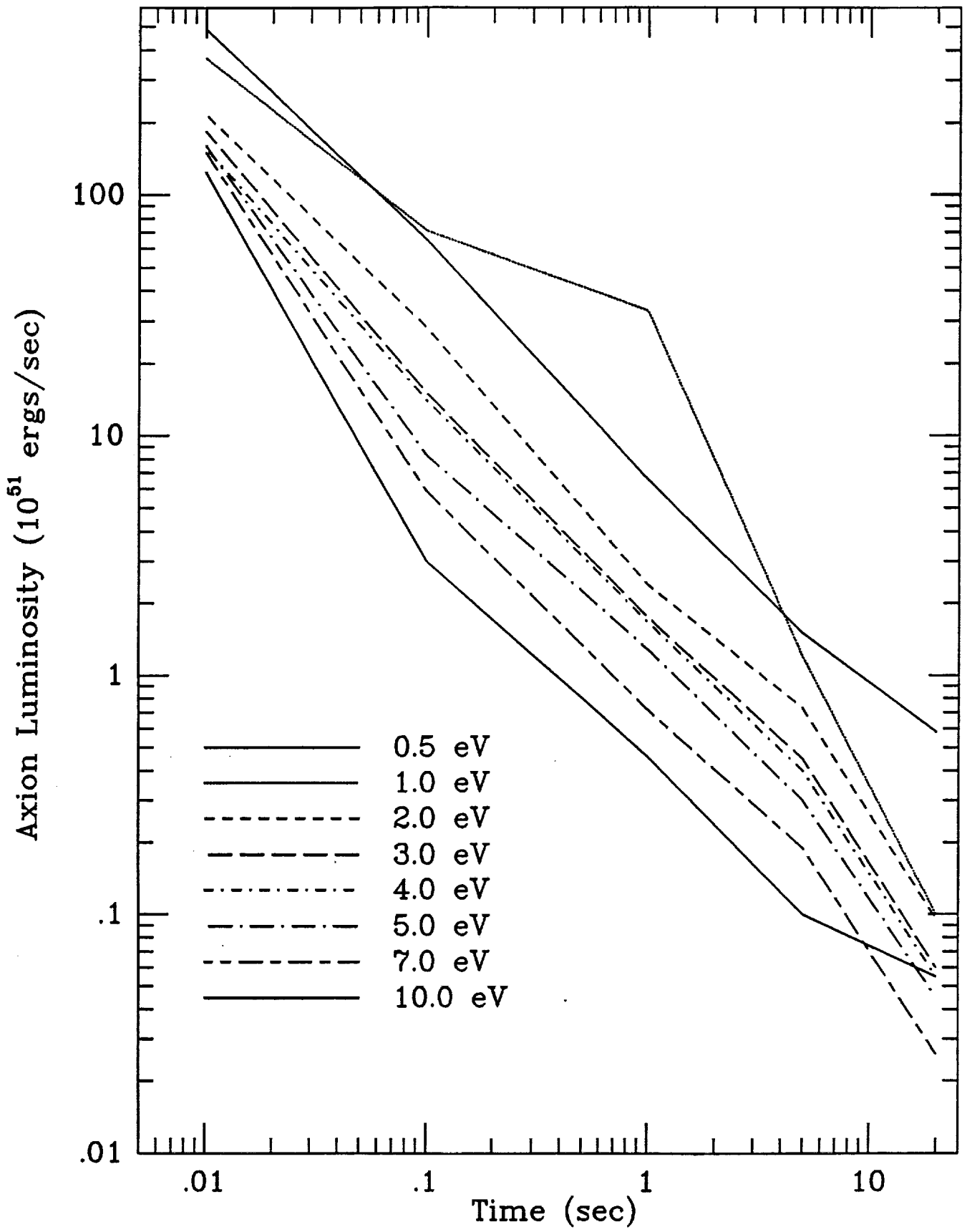


Figure 6

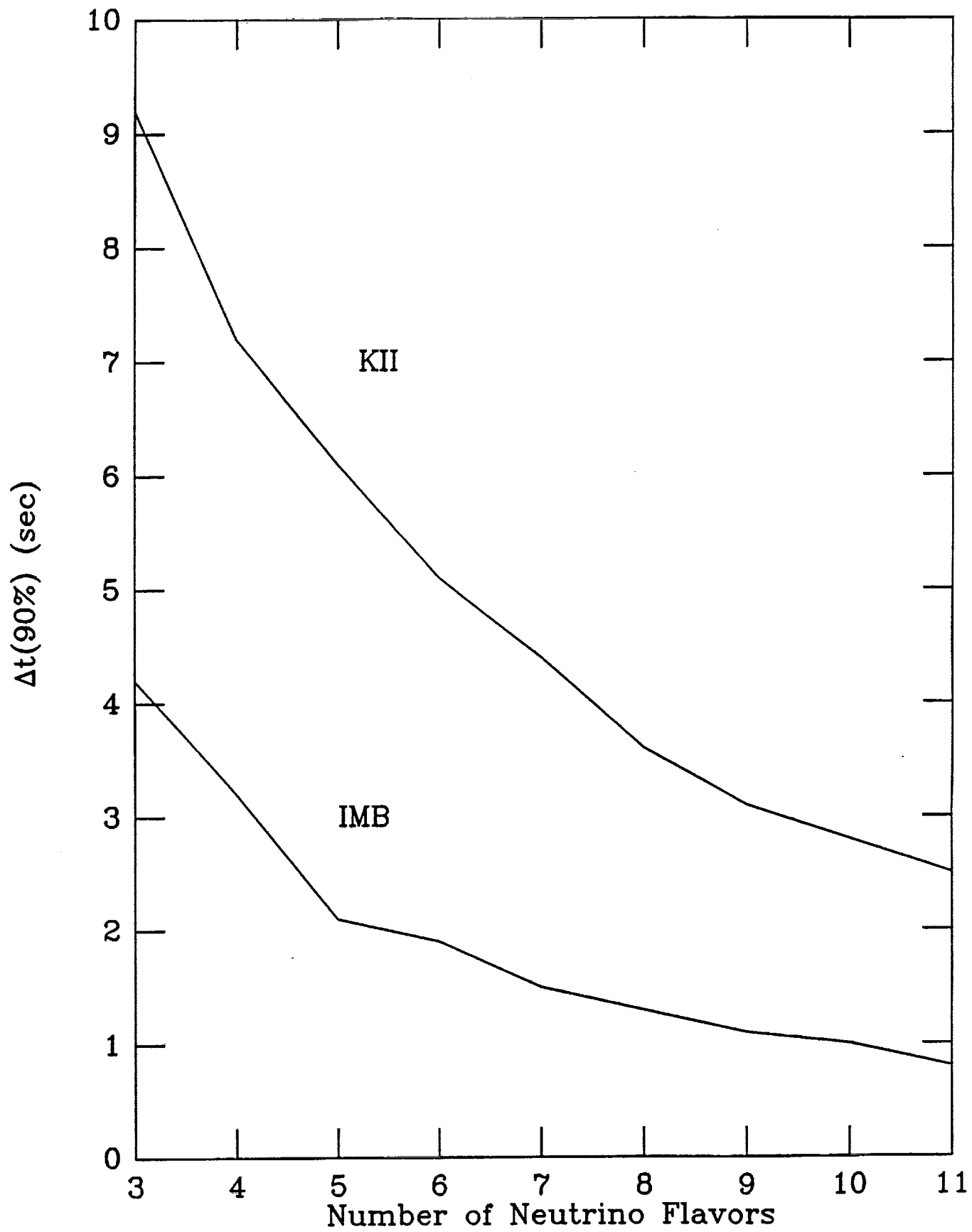


Figure 7

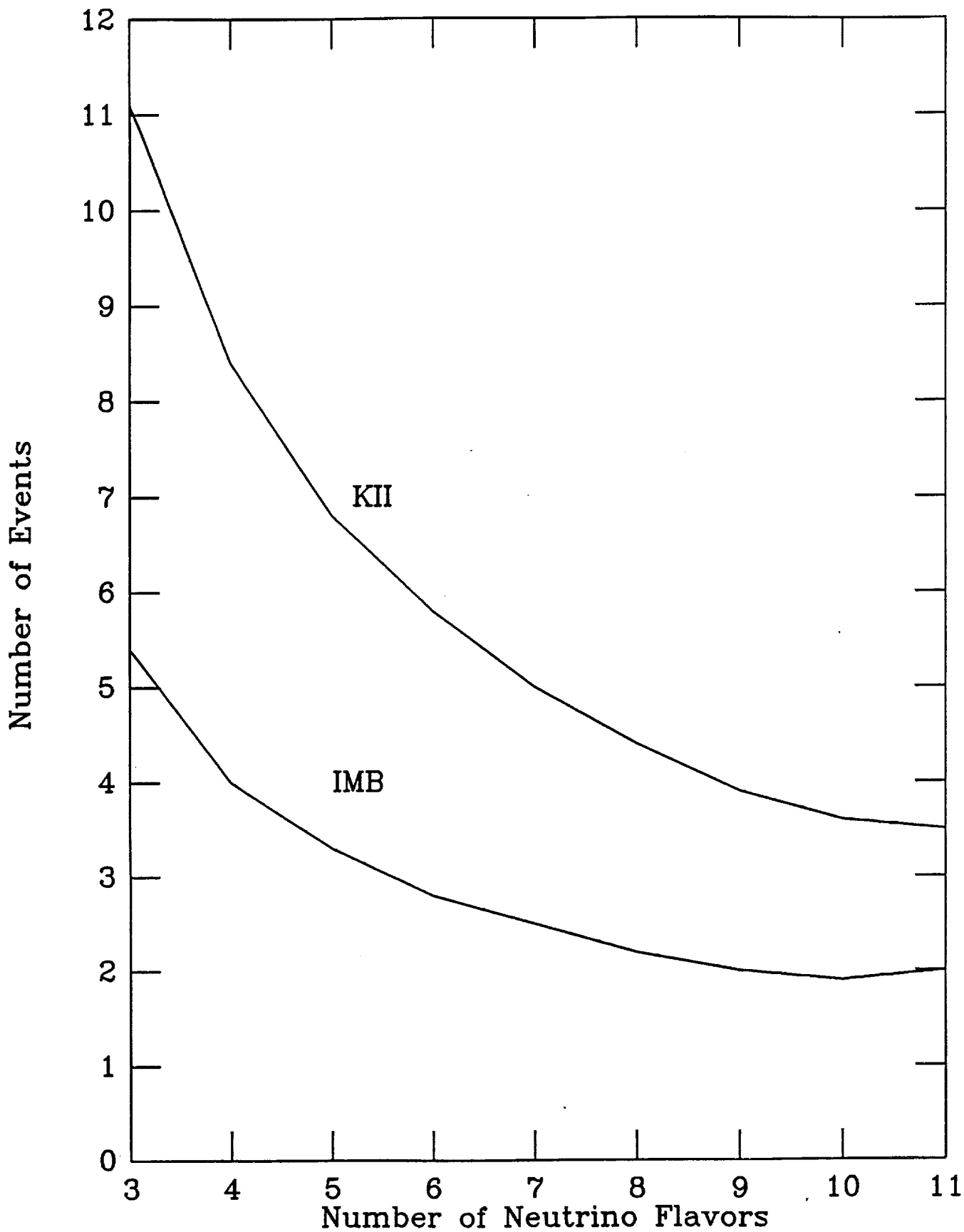


Figure 8

